

SGIDN-LCD: An Appearance-based Loop Closure Detection Algorithm using Superpixel Grids and Incremental Dynamic Nodes

Baosheng Zhang

Abstract—Loop Closure Detection (LCD) is an essential component of visual simultaneous localization and mapping (SLAM) systems. It enables the recognition of previously visited scenes to eliminate pose and map estimate drifts arising from long-term exploration. However, current appearance-based LCD methods face significant challenges, including high computational costs, viewpoint variance, and dynamic objects in scenes. This paper introduces an online based on Superpixel Grids (SGs) LCD approach, SGIDN-LCD, to find similarities between scenes via hand-crafted features extracted from SGs. Unlike traditional Bag-of-Words (BoW) models requiring pre-training, we propose an adaptive mechanism to group similar images called *dynamic node*, which incrementally adjusts the database in an online manner, allowing for efficient retrieval of previously viewed images. Experimental results demonstrate the SGIDN-LCD significantly improving LCD precision-recall and efficiency. Moreover, our proposed overall LCD method outperforms state-of-the-art approaches on multiple typical datasets.

Index Terms—Loop closure detection (LCD), SLAM, place recognition, Superpixel Grids

I. INTRODUCTION

The development of autonomous mobile robotics and augmented reality has garnered significant attention in the field of simultaneous localization and mapping (SLAM). SLAM utilizes various sensors to construct precise maps of unknown environments and incrementally localize itself without any prior information. While LiDAR and camera have been the primary sensors used for SLAM in recent years, visual SLAM has emerged due to the rapid advancement of computer vision and the availability of low-cost visual sensors. Nevertheless, irrespective of the sensor type, there are inevitable sources of noise that generate inaccurate measurements, resulting in inconsistent representations when considering only raw sensor data. Wherein, visual SLAM systems are particularly affected by viewpoint variance, dynamic objects, and the layout changes commonly found in indoor scenes. These factors can cause accumulated errors during long-term and large-scale mapping and localization processes. To address these challenges, Loop Closure Detection (LCD) module has been introduced into SLAM systems. LCD enables robots to correctly identify previously-seen scenes, reducing drift and improving the accuracy of SLAM systems.

The problems of appearance-based visual LCD is an important research topic in robotics and computer vision. Despite notable differences, it can be viewed as an online visual place recognition (VPR) task. While LCD prioritizes real-time performance and recognition accuracy. Typically, LCD methods

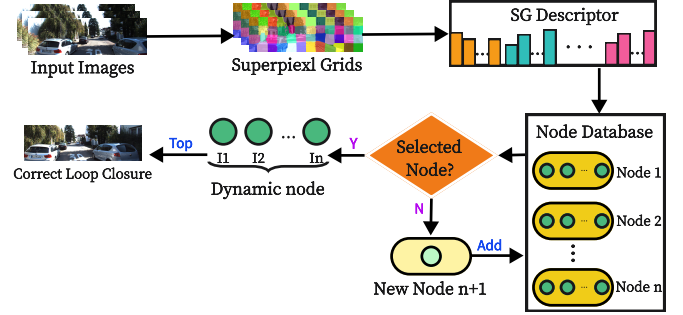


Fig. 1. Basic overview of SGIDN-LCD. The SGIDN-LCD approach consists of four main parts: Superpixel Grid Segmentation, Hand-Crafted Descriptor extraction, similarity calculation, and dynamic node selection.

consist of two stages: feature extraction and candidate frame selection. The former aims to represent scenes effectively and robustly, which has been advanced by the development of efficient binary descriptors such as BRIEF [1], ORB [2], LDB [3], and AKAZE [4], as well as traditional point features like SURF [5] and SIFT [6]. Visual words are then generated via quantization of the space of local descriptors. Bag-of-Words (BoW) [7] approach utilizes the widely-used term frequency-inverse document frequency (TF-IDF) technique to construct a visual word histogram and combines it with the inverted index method to rapidly calculate similarity between the current query image and previous images for identifying potential loop closure pairs, i.e., candidate frames.

Despite the overall effectiveness of existing BoW-based LCD methods, several challenges still need to be addressed. Firstly, the conventional BoW framework relies solely on the distribution of local hand-crafted features and neglects the spatial relationships between visual words in scenes, making it vulnerable to being misled by scenes containing many similar objects. Secondly, the requirement for a pre-trained module for database visual vocabulary can be time-consuming and lead to false loop detection when querying datasets with different appearance types from the training image sets. These issues call for further research efforts to enhance the performance and robustness of LCD methods in practice.

In this paper, we propose an online visual LCD algorithm based on Superpixel Grids (SGs) to improve accuracy and recall performance. Our approach utilizes SG segmentation to generate adaptive irregular grids for scene factors and create local SG features based on pixel intensities for each grid in a scene. The similarity between query and database images

is calculated using SG features, taking into account both the local characteristics of the image and the relative positional relationship between features. Additionally, we introduce a novel concept of *dynamic node* that search for previously visited similar images and reduce processing times. Unlike previous methods [8] [9], our approach adaptively guides new images to select the correct node or build a new node to group similar input images. This enables our algorithm to efficiently handle changes in the environment and improve its performance over time.

To summarize, the main contributions of this paper are as follows:

- We propose a novel feature extraction approach for image representation, which is based on SG segmentation. Our approach leverages local spatial characteristics to enable efficient similarity calculation between images. This mitigates the adverse effects of significant appearance changes and improves precision and recall performance.
- A novel concept, *dynamic node* has been proposed for adaptive dynamic grouping similar previously visited images and selected candidate frames to reduce processing time.
- A complete LCD approach with improved precision-recall performance and time efficiency is proposed and evaluated on eight challenging sequences.
- A new indoor dataset recorded, which include strong lighting changes and severe appearance changes, with typical loop-closure. Our datasets are available at <https://drive.google.com/drive/folders/1-tRfQ3cKriTVYb2mmEyF45Ij1mHpRjkX?usp=sharing>

The rest of this paper is organized as follows. Section II provides a brief overview of related works on LCD methods. In Section III, we describe proposed algorithm in detail, highlighting its key features and advantages. To evaluate the performance of our approach, comparative experiments with state-of-the-art LCD algorithms are presented in Section IV. Finally, we summarize our findings and discuss future work in Section V.

II. RELATED WORK

The appropriate feature selection and rational utilization of extracted features are critical for achieving accurate identification of visited location scenes, as well as robustness against viewpoint variations and strong appearance changes in dependable LCD methods. This section provides a concise overview of algorithms related to image features and other relevant approaches utilized in SGIDN-LCD.

A. Hand-Crafted Features for LCD

Image representation is a crucial aspect of appearance-based LCD algorithms. Most methods utilize feature sets to reduce image dimensionality and express scenes efficiently. For example, Fast Appearance-Based Mapping (FAB-MAP) [10] extracts SURF point features from query images and clusters them into visual words using k-means in low-dimensional space. A Chow-Liu tree approximates the probabilities of

visual word co-occurrence for fast similarity evaluation between query and database images. Other feature extractors such as SIFT [6], KAZE [11], BRIEF [1], and ORB [2] have also been proposed for various scenes. However, these hand-crafted features have limitations, including high computational resource requirements, low robustness, and susceptibility to matching errors caused by noise and deformation in images.

B. Feature Integration and Encoding Optimization

To address these challenges, research has been focused on how to integrate extracted features to preserve image characteristics and enable fast and accurate loop closure detection. BoW models group similar visual words for direct matching of BoW descriptors. However, visual words generated by clustering image features using k-means or k-medoids tend to lose geometric information between features in images [12–15], which may limit their expressive ability in complex scenes.

To address this issue, researchers have introduced temporal or spatial consistency constraints into LCD. Recently, many studies have attempted to improve querying performance by using vectorized representations such as Vector of Local Aggregated Descriptors (VLAD) [16, 17] and Fisher Vectors (FV) [18], or by employing voting approaches such as Hierarchical Navigable Small World (HNSW) [19]. These works aim to encode and match visual features more effectively to enhance loop closure detection performance.

C. Addressing Appearance Changes in Place Recognition

The quantity of methods for place recognition in changing environments is rapidly expanding. However, no consistent solution has been presented for the practical challenge of detecting severe appearance changes and changing viewpoints. Some approaches to address this problem is to use fixed patches to detect repetitive features. Naseer *et al.* [20] proposed a graph theoretical approach that formulates image matching as a minimum cost flow problem in a data association graph. To calculate image similarity, they used a dense, regular grid of Histogram of Oriented Gradients (HOG) descriptors and generated multiple route matching hypotheses by optimizing network flows. Milford *et al.* [21] selected candidate frames based on whole image matching and verified correct loop-closure using local image regions. Although this method can reduce false positive matches, it cannot increase the number of matches when there are viewpoint changes.

Recently, combining Convolutional Neural Network (CNN)-based descriptors and local region detectors has been employed to increase robustness towards viewpoint changes [22, 23]. EdgeBoxes [24] was utilized as an object proposal method to detect local regions in [22], while several local region detectors including SIFT [6], two object proposal methods [25, 26], and a segment soup [27] were combined with CNN-based descriptors in [23]. Preliminary results suggest that this combination shows promise, however, it still needs improvement regarding repeated detection of local image regions in the presence of severe environmental changes.

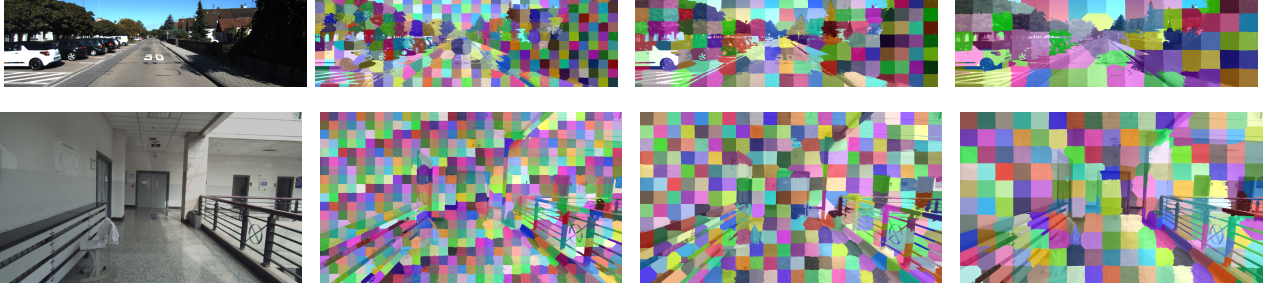


Fig. 2. The top and bottom parts of the images respectively depict outdoor scenes (from the KITTI dataset) and indoor scenes (from the NEU dataset). Superpixel Grid Segmentation was performed on these images using various segmentation scales. The resulting segmentation highlights the variability in optimal scale selection for different scene categories.

This paper presents SGIDN-LCD, an online and efficient visual LCD approach that is suitable for handling severe appearance and viewpoint changes. The proposed approach employs the Superpixel Grid algorithm to segment scenes into multiple semantic regions, each containing local information. We extract SG features based on pixel intensity to encode each image and enhance system robustness and performance. To further improve efficiency, we introduce *dynamic node* to group images with similar appearances, reducing processing time for loop closure detection. Our experiments demonstrate that this approach yields significant improvements in both precision-recall performance and efficiency, especially when dealing with large-scale datasets.

III. TECHNICAL APPROACH

A. Overview

Figure 1 provides an overview of SGIDN-LCD approach. It comprises four main components: Superpixel Grid Segmentation based on local appearance characteristics, Hand-Crafted Descriptor extraction, similarity calculation, and dynamic node selection. Unlike most state-of-the-art visual LCD approaches that rely on BoW, our system does not require offline or online training stages and the use of a trained large-scale visual dictionary. This advantage reduces physical memory needs and running times.

Our approach involves several key components. Firstly, we implement the Superpixel Grid method, which divides the current scene into multiple ($M \times N$) irregular grids with local scene information. This method is inspired by the Simple Linear Iterative Clustering (SLIC) algorithm [28] and helps to address the adverse effects of changes in the environment on implementation effectiveness. In Section III-C, we provide details of our local feature extraction based on SGs, which involves extracting features from both the segmented SGs as mentioned above and the pixel intensities of the image. Furthermore, we analyze in detail the advantages of SG feature over traditional point features from various perspectives. Next, we calculate the similarity between query and database images. To efficiently search previously visited scenes and select candidate frames, we provide a detailed introduction to the working principle of the *dynamic node* in Section III-D. By identifying the image with the highest similarity to the query

image in the selected candidate frames, we can determine the correct loop-closure.

The following subsections will provide additional details on our proposed method.

B. Superpixel Grid Segmentation

When a scene contains dynamic objects or severe viewpoint changes, the performance of an LCD system may significantly degrade. In feature-matching methods, local features have been demonstrated to be more robust to appearance changes than global features and are therefore widely used in image representation. In this paper, we propose a Superpixel Grid Segmentation method based on the SLIC framework, which divides an image into irregular grids based on local features.

To obtain SGs with high resilience, we first convert an image to grayscale and initialize images with fixed grids of various sizes, selecting uniformly distributed center points of the fixed grids as the initial center of the SGs before performing Superpixel Grid Segmentation. In this process, the segmentation scale, which refers to the size of the initialized fixed grid, is defined as S_p . Additionally, we define the fuse distance, denoted as F_d , between the center and other points in the SG. This distance is calculated based on both Euclidean distance d_e and pixel intensity difference d_i , as follows:

$$\begin{aligned} d_e &= \sqrt{(x_c - x_i)^2 + (y_c - y_i)^2} \\ d_i &= \sqrt{(p_c - p_i)^2} \\ F_d &= \sqrt{\left(\frac{d_e}{n}\right)^2 + \left(\frac{d_i}{m}\right)^2} \end{aligned}$$

In these equations, d_e and d_i represent the Euclidean distance and pixel intensity difference between the SG center and other points in the same SG. The variables (x_c, y_c) and (x_i, y_i) denote the locations of the center and local region points in the SG, and p_c and p_i represent their respective pixel intensities. The range of values for x_i and y_i are $(x_c - S_p, x_c + S_p)$ and $(y_c - S_p, y_c + S_p)$, respectively. Finally, F_d represents the fuse distance between the center and other points within the same SG. The center point of each grid is iteratively updated using the k-means algorithm until robust SGs are obtained.

Scene segmentation can be performed at multiple scales to address various types of scenes. Generally, more precise segmentation can better preserve the image information, however, it also requires more running time and memory resources. Figure 2 demonstrates an example image with different values of S_p for both outdoor and indoor scenes. It is evident that outdoor open scenes, such as those shown in the upper images, are better suited for larger values of S_p . Conversely, complex indoor scenes, like those displayed in the lower images, work better with a smaller value of S_p .

C. Hand-Crafted Descriptor Extracting

Repeatability and accuracy are essential in local feature extraction algorithms, where the feature descriptors play a critical role. Moreover, the feature extractor should be time-efficient to meet real-time requirements. In this regard, we propose an effective and straightforward feature based on SGs to represent image information and participate in subsequent tasks. This section will provide a detailed introduction to the properties of this feature.

To achieve real-time performance and efficiently represent images using limited computational resources, we utilize Superpixel Grid Segmentation and calculate patch-level descriptors called Local Superpixel Grid Descriptor (LSGD), which encode the content of pixel intensity in each SGs. Specifically, at this stage, the current image is represented as a histogram of words with dimensions $M \times N \times 256$, as illustrated in Figure 3. Here, M and N denote the number of grids that were segmented in Section III-B. The similarity *simScore* between images is defined as follows:

$$\text{simScore} = \sum_{i=1}^M \sum_{j=1}^N L_1(\text{LSGD}_Q(i, j), \text{LSGD}_B(i, j))$$

where L_1 represents the distance of the L1 norm and $\text{LSGD}_Q, \text{LSGD}_B$ denote the LSGD descriptors of query and database images, respectively.

This approach effectively overcomes the deficiencies of traditional feature descriptors such as SURF, SIFT, and ORB in practical application scenarios. Firstly, the LSGD code efficiently encodes all pixels while preserving more information of the image without requiring complex pixel-level operations that consume significant computation time. Furthermore, the use of local pixel intensity based on SGs greatly reduces the impact of dynamic objects and viewpoint changes. Secondly, the LSGD feature descriptor of each SG avoids uneven distribution of features in complex scenes, thereby improving the performance of LCD approaches. Finally, the use of patch-level descriptors reduces the occurrence of false matches, which are common in traditional feature descriptors extracted from current images, significantly improving the accuracy of visual systems.

D. Building and Selecting Dynamic Node

Most visual LCD methods based on the BoW model require a training stage. In this work, we propose an incremental online approach to overcome this issue by creating image

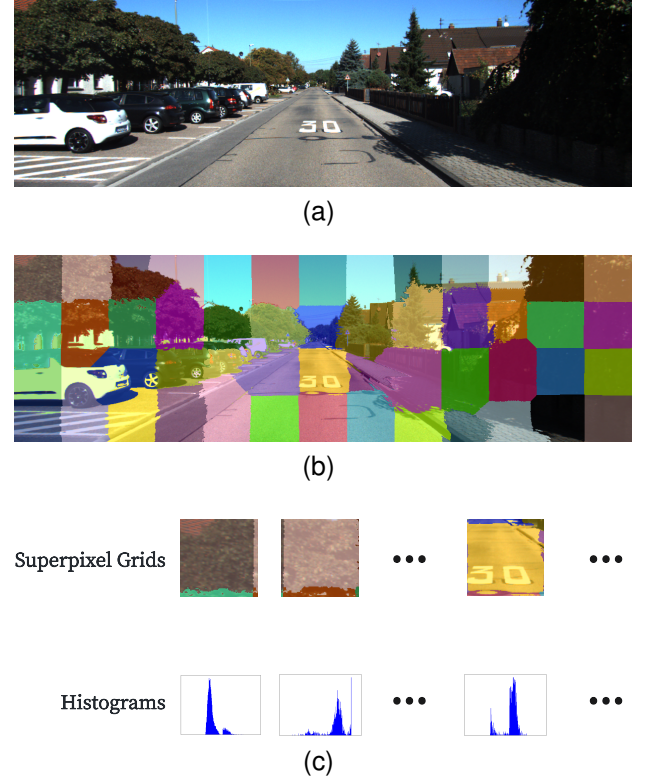


Fig. 3. Illustrates the process of extracting LSGD features from an input query image on the KITTI-05 dataset. The example image is shown in (a), and its SG representation obtained through Superpixel Grid Segmentation is illustrated in (b). The LSGD descriptors are then extracted from the segmented grids, as shown in (c).

groups (i.e., *dynamic nodes*). By doing so, we fundamentally address the challenges that pre-trained models, such as BoW-based methods, may face when encountering input scenes that differ from those used in the training phase. Furthermore, the *dynamic node* concept can improve efficiency of the system. Once the current frame I_c meets the similarity requirements of the corresponding node, the traversal process will be terminated, and the system will directly move to the current loop closure verification step. As a result, it is not necessary to traverse every image in the dataset, which saves computational resources and reduces processing time.

As described in the Section III-C, we have extracted LSGD. To efficiently select and construct similar image groups based on scene information, we utilize a second-order similarity estimation strategy in node selection. For the current query image I_c , we calculate its appearance similarity with the first image, I_{i1} , in all existing image groups (nodes) ranging from N_1 to N_n based on their LSGD. If the similarity score S_{k1} for the k th node is greater than the predefined threshold α , we consider the image group as a candidate node and evaluate the similarity between I_c and all images in the image group (I_{k1}, \dots, I_{km}). When the average similarity score S_{ave_k} between I_c and all frames in this node reaches the predefined threshold β , all images in this candidate node will join the subsequent loop-closure determination as candidate frames. Then, image I_c will be added to the selected node as a new group frame to participate in analyzing and selecting similar

image groups for future input of new images. Notably, if all similar image groups have been traversed and no nodes meet the similarity requirement, a new node will be created, and I_c will become the only frame, waiting for subsequent input images that meet the requirements, to gradually extend the size of the group, as depicted in Figure 1. The detailed process of *dynamic node* is summarized in Algorithm 1.

Algorithm 1 : Outline of the *dynamic node* algorithm

Input: The LSGD descriptor of I_c and all previous visited images.

Output: The selected *dynamic node*.

```

1: for  $i = 1 : n$  do
2:    $S_{i1} = \text{SimLSGD}(I_c, I_{i1})$ 
3:   if  $S_{i1} > \alpha$  then
4:     for  $j = 1 : m$  do
5:        $S_{ave_i} += \text{SimLSGD}(I_c, I_{ij})$ 
6:     end for
7:      $S_{ave_i} /= m$ 
8:     if  $S_{ave_i} > \beta$  then
9:        $I_c$  insert to node  $N_i$ 
10:      return dynamic node  $N_i$ 
11:     end if
12:   end if
13: end for
14: new dynamic node  $N_{n+1}$  from  $\text{NodeBuilding}(I_c)$ 
15: return dynamic node  $N_{n+1}$ 

```

E. Loop Closing Verification

Following the aforementioned process, images belonging to the same node typically exhibit high similarity to each other, suggesting that they are likely located in the same local spatial position. To further utilize this observation, we can select the top N images with the highest similarity to the current query frame I_c to participate in subsequent algorithmic processes or choose the image with the highest similarity to I_c as the final loop closure frame.

IV. EXPERIMENTAL RESULTS AND ANALYSIS

To evaluate the effectiveness of our proposed LCD algorithm, SGIDN-LCD, a series of experiments were conducted. This section first outlines the datasets used, then analyzes the performance of the LSGD, as well as the results of testing the *dynamic node* database architecture using our method. In addition, we present qualitative and quantitative results to demonstrate the superior performance of our approach with state-of-the-art LCD algorithms.

The experimental setup involved testing the program on a laptop equipped with Ubuntu 18.04 operating system, an Intel i7-10510U CPU @ 1.80GHz \times 8, and 8GB RAM.

A. Datasets

To evaluate the performance of SGIDN-LCD, we conducted experiments on four standard datasets:

- The City Centre dataset [10] was collected using a mobile robot equipped with two cameras pointing in opposite

directions. The robot completed two laps of a 2 km loop, resulting in 2474 images along with GPS positioning data. This dataset contains dynamic objects such as cars and pedestrians, which pose a challenge for LCD algorithms.

- The New College dataset [10] was also collected by a robot traversing a complex trajectory of 1.9 km with many loop closures. The dataset consists of 2146 images. Illumination changes and repeated patterns in the dataset are the main factors that decrease the performance of LCD algorithms.
- The KITTI dataset [29] is a well-known binocular outdoor dataset consisting of 22 image sequences with a total of 44182 images and a trajectory length of 39.2 km. Ground truth trajectories are provided for 11 out of the 22 sequences. Illumination and viewpoint changes are present in this dataset, and we used the KITTI00, KITTI05, and KITTI06 sequences in our experiments.
- The NEU dataset was gathered in indoor scenarios using a handheld binocular camera and includes 4 image sequences with a total of 4733 frames collected. It is a suitable benchmark for various computer vision tasks. We used the YF and HSL sequences with loop closures to estimate the performance of our method.

B. Effectiveness of LSGD Features

Before evaluating the proposed LCD performance, we first verify the effectiveness and efficiency of LSGD features utilize a typical precision-recall metric. Precision is defined as the ratio between the number of true positive closed loops and the total number of closed loops detected by the algorithm. On the other hand, recall is defined as the number of true positive closed loops over the total number of loop closure events defined in the ground truth. False positive loop closure is intolerable for the SLAM system because it may lead to deviation in the final positioning result. Hence, we set the precision rate to 100% and evaluate with maximum recall rates. Additionally, we used the maximum precision rates at 100% recall to evaluate the performance of our approach as a candidate frame selection method. We also compared the average execution time for different segmentation scales on eight datasets using the same platform. The results are presented in Figure 4.

Subsequently, we compared our approach with four state-of-the-art feature-based LCD algorithms, namely DBoW [7], iBoW [8], FAB-MAP [10], and SRLCD [30]. We implemented these algorithms based on publicly available codes and tuned the parameters to achieve their best possible performance.

1) *LCD with Different Segmentation Scales*: In this section, we explore the impact of segmentation scale S_p on the maximum precision rate and maximum recall rate at 100% recall and 100% precision, respectively, for our proposed method. To this end, we conducted a series of experiments by gradually increasing S_p from 10 to 100 with a step size of 10, and the results are presented in Figure 4. As shown in Figure 4(a) and (b), it is observed that the maximum precision rates and maximum recall rates of all sequences show an initial

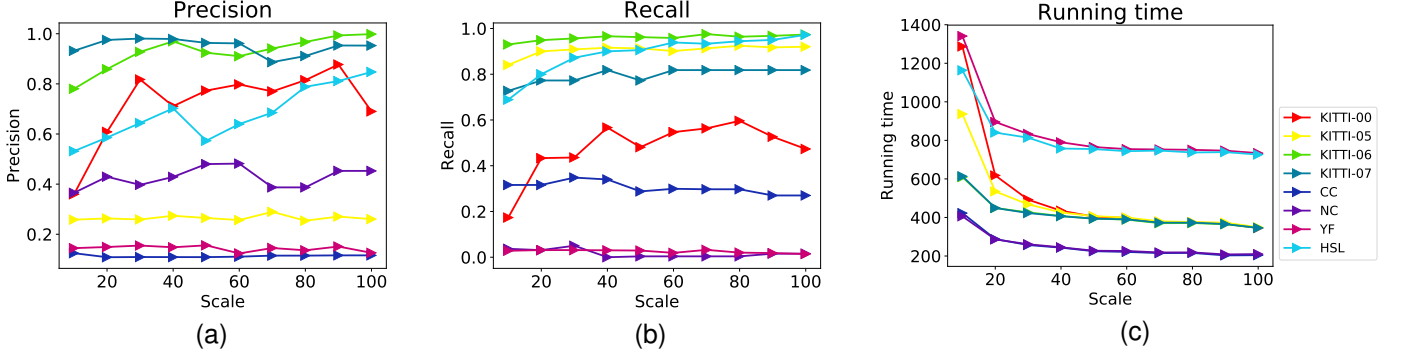


Fig. 4. The performance of the LSGD with different segmentation scales in terms of maximum precision (%), maximum recall (%) and running time (ms) on the eight image sequences.

TABLE I
COMPARISONS OF DIFFERENT LOOP CLOSURE DETECTION APPROACHES

Dataset	#Images	Metric	DBoW	iBOW	FAB-MAP	SRLCD	LSGD
KITTI-00	4541	Recall (%)	4.84	24.38	22.40	46.91	56.67
		Precision (%)	80.92	2.20	2.20	2.20	71.10
		Time (ms)	1415.106	154.811	69.588	284.518	435.176
KITTI-05	2761	Recall	83.91	49.42	31.44	38.84	91.59
		Precision	43.93	3.71	3.71	3.71	27.37
		Time	958.348	134.733	82.578	200.289	426.042
KITTI-06	1101	Recall	88.86	48.67	33.77	37.16	96.60
		Precision	93.65	9.47	9.47	9.47	96.97
		Time	528.610	103.542	127.157	108.083	407.396
KITTI-07	1101	Recall	95.45	50.00	13.63	22.72	81.81
		Precision	99.77	6.74	6.74	6.74	97.91
		Time	452.316	100.817	128.065	102.633	406.689
City Centre	1237	Recall	14.70	34.30	-	0.62	33.99
		Precision	8.66	8.66	8.67	8.66	10.89
		Time	452.708	85.691	110.751	21.018	243.257
New College	1073	Recall	0.58	-	-	-	-
		Precision	9.89	9.37	9.37	9.37	42.88
		Time	409.133	82.945	124.883	21.435	245.241
YF	1415	Recall	0.40	-	-	-	3.02
		Precision	44.23	7.42	7.42	7.42	14.81
		Time	552.259	121.468	110.875	53.672	790.051
HSL	968	Recall	46.11	46.11	12.77	-	90.00
		Precision	77.82	10.26	10.26	10.26	70.24
		Time	409.090	107.438	139.462	50.619	757.712

The (-) symbol indicates that the approach did not achieve 100% precision or recall rates on the given dataset. Consequently, it is not possible to calculate the corresponding maximum recall or precision rates at 100% precision or recall rates.

increasing trend with increasing S_p before stabilizing. This behavior can be attributed to the fact that an appropriately large S_p allows for the inclusion of complete scene factors in the same SGs, which is a key factor in accurately calculating image similarity. Additionally, the average execution time gradually decreases with an increasing S_p before stabilizing.

Based on our experimental analysis, we select $S_p = 40$ as the optimal segmentation scale for use in our subsequent experiments.

2) *Comparison With the Other Approaches:* To evaluate the precision-recall performance and efficiency of the proposed LSGD features, we analyzed the maximum recall rates and maximum precision rates at 100% precision and recall, respectively, as well as the average execution time for different state-of-the-art approaches. As shown in Table I, the LCD approach with LSGD outperforms most sequences in terms of maximum recall at 100% precision, showing an improvement

by an average of 244.4% compared to the previous best method DBoW. In addition, the maximum recall rates were about 20.8% and 95.2% higher than suboptimal methods in the typical outdoor sequence KITTI-00 and indoor sequence HSL, respectively. For maximum precision rates at 100% recall, which ensures the final implementation effect of the LCD method when selecting candidate frames, the LSGD method achieved state-of-the-art results compared to the DBoW. Even in some scenes, our method demonstrated better performance than state-of-the-art approaches in terms of precision.

Regarding time complexity, although the proposed method did not achieve the best performance compared to state-of-the-art methods, the time complexity of LSGD does not significantly increase with an increase in input images. This characteristic shows significant advantages in real-time loop detection of large scenes. As presented in Table I, the average running times increased by approximately 47.6%, 14.9%,

TABLE II
PERFORMANCE OF DYNAMIC NODE APPROACH

Dataset	β	#Nodes	LSGD + dynamic node				LSGD			
			Times	R@1	R@5	R@10	Times	R@1	R@5	R@10
KITTI-00	0.9	91	363.267	66.27	86.68	88.46	435.176	98.81	99.26	99.55
	1.0	150	360.015	71.59	94.82	96.30				
	1.1	1972	364.504	81.65	81.65	81.65				
KITTI-05	0.9	65	377.541	40.86	61.44	66.37	426.042	96.52	97.39	97.39
	1.0	113	366.545	46.95	61.73	65.50				
	1.1	1246	380.418	62.89	62.89	62.89				
KITTI-06	0.9	22	359.468	70.15	91.08	92.63	407.396	100.00	100.00	100.00
	1.0	31	344.248	67.05	92.24	93.79				
	1.1	453	368.831	70.93	71.31	71.31				
KITTI-07	0.9	28	410.403	0.00	9.09	9.09	406.689	72.72	72.72	81.81
	1.0	47	406.105	0.00	18.18	27.27				
	1.1	537	429.395	9.09	9.09	9.09				
City Center	0.9	7	299.273	52.05	86.00	94.44	243.247	89.30	96.70	98.14
	1.0	11	257.258	52.05	85.59	93.62				
	1.1	353	215.809	39.91	45.47	48.35				
New College	0.9	8	196.907	72.75	97.43	98.71	245.241	89.74	99.03	99.35
	1.0	9	211.941	73.39	97.43	98.07				
	1.1	238	187.406	61.53	76.60	77.24				
YF	0.9	88	720.484	21.69	67.33	79.80	790.051	75.81	85.53	93.01
	1.0	122	708.232	24.18	65.08	76.55				
	1.1	648	704.158	9.72	9.97	9.97				
HSL	0.9	62	724.432	34.52	71.42	75.00	757.712	92.85	92.85	94.04
	1.0	104	768.909	39.28	64.28	64.28				
	1.1	459	692.633	23.80	25.00	25.00				

and 42.0% in DBoW, iBoW, and SRLCD, respectively, from KITTI-05 with 2761 frames to KITTI-00 with 4541 frames. However, the running time of LSGD only increased by 2.0%.

C. Effectiveness of Dynamic Image Node

To evaluate the performance of our dynamic node framework, we conducted a comparative experiment for LCD methods that utilize different database architectures. We evaluated the recognition performance mainly based on Recall@N, whereby a query is regarded as correctly localized if at least one of the top N retrieved database images is within the ground truth tolerance. We recorded the running time and recognition performance of LSGD based on *dynamic node* with different threshold values of β , as shown in Section III-D, and the results are presented in Table II. To analyze the influence of β values on the dynamic node in terms of running time, we varied its values to 0.9, 1.0, and 1.1. We observed that the average minimum execution time per frame when β was set to 1.0 and 1.1. Large β values usually consist of fewer images in each node, and the method's execution time is influenced by the process of computing average similarity score and the number of computed nodes. Therefore, selecting the optimal image number in each node, i.e., the optimal β , can keep the speed up of the LCD method process. Subsequently, we compared the results of standard LSGD with the method using *dynamic node*, as shown in Table II. It is noteworthy that the method using *dynamic node* outperforms on all datasets in terms of average execution time, with an average improvement of 11.93%, 4.30%, and 4.56% (absolute improvement for $\beta = 1.0$).

Furthermore, we studied how the β value affects the recognition performance of LCD by comparing method based on

dynamic node framework with different β values and a standard LSGD without *dynamic node*. It is noteworthy that *dynamic node* only retains previously seen images for similarity calculation with the current query image, and the images that are later than the current image are not included into nodes. Therefore, the recognition of image functionality in this part is based solely on the previous images' recognition function of the current image. As shown in Table II, the best performance was generally achieved at β equal to 0.9 and 1.0. As mentioned above, β directly affects the number of images in each node, and large β values usually result a small number of images in each node, which may cause the query image to be collected in the nearby incorrect similar dynamic node. For traditional methods, there is a degradation in performance compared to the *dynamic node* since highly similar nodes attract the query image before finding the correct pair image.

After the above analysis, the *dynamic node* method can significantly improve the running efficiency while maintaining high-level or similar recognition performance to traditional methods.

D. Comparative Results

In this section, we present a comprehensive evaluation of our proposed LCD method by providing both quantitative and qualitative analyses of loop closure detection precision-recall and overall performance compared to state-of-the-art LCD algorithms.

To begin with, we compared our approach against four public state-of-the-art LCD schemes on eight datasets using precision-recall curves, as shown in Figure 5. The results demonstrate that the LSGD outperforms other methods on these datasets, particularly the outdoor KITTI and FAB-MAP

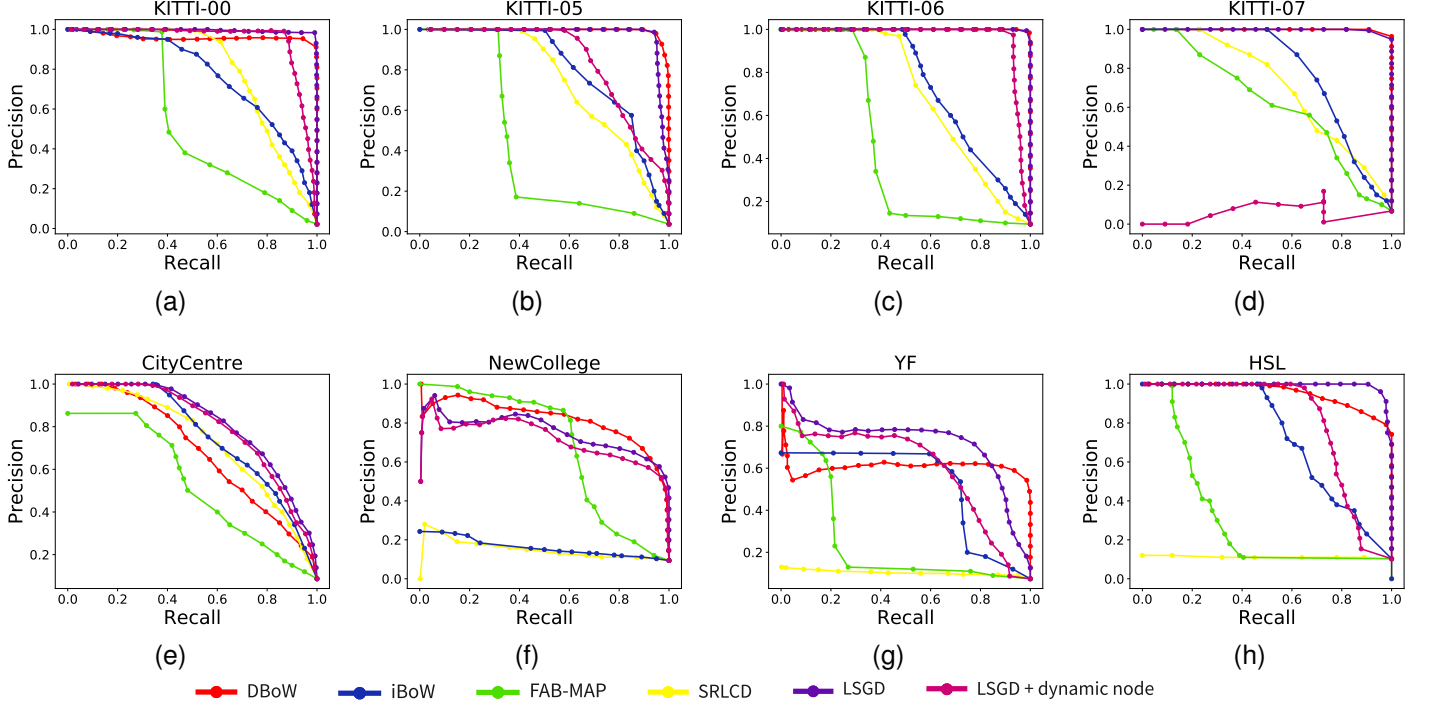


Fig. 5. The comparison of the precision-recall curves between LSGD and state-of-the-art LCD methods, like DBoW, iBoW, FAB-MAP and SRLCD on the outdoor and indoor sequences. From top to bottom, left to right: KITTI-00, KITTI-05, KITTI-06, KITTI-07, City Centre, New College, YF and HSL.

datasets. This is because the key scene factors used for recognition in outdoor scenes can be more effectively divided by methods based on grid segmentation models. Furthermore, the LSGD-based method produces better implementation results than other point feature-based LCD methods via key scene factors to improve recognition performance and reduce dynamic objects affection the task.

However, in Figure 5 (d), we observed performance degradation when the LSGD method with *dynamic node* on KITTI-07. Due to the scattered distribution of correct loop closure images in the dataset, which made it challenging to include correct loop closure images in the same nodes. In contrast, correct loop closure images were tightly distributed in KITTI-06, City Centre, and New College, with dynamic nodes adjacent to each other. Therefore, the performance of the LSGD method with *dynamic node* framework basically reached the level of standard LSGD in the KITTI-06 and FAB-MAP datasets.

To provide a more comprehensive analysis of the performance of our LCD algorithm, we further evaluated the system's precision, recall, and running time. We define a comprehensive evaluation score PRT as below.

$$PRT = AUC / (1 + \omega * RunningTime(s))$$

, wherein AUC denotes area under the precision-recall curve score, the ω is set to 10.0 in this work. We conducted a comparative experiment using different LCD approaches on eight sequences and present the results in Figure 6. Our findings demonstrate that the LSGD method outperforms all other experimental methods in the KITTI dataset, with particularly notable improvements observed in the KITTI-00 and

KITTI-05 sequences. Specifically, in terms of PRT , the LSGD method achieved an improvement of 146.1% and 94.1% on average compared to other approaches. This was evidenced by two aspects: firstly, the LSGD method produced the best precision-recall performance in the outdoor KITTI dataset as shown in Figure 5. Secondly, in terms of running time, LSGD maintained a relatively stable trend as the number of images increased, thereby providing better average execution time performance in the KITTI dataset with a large number of images. As for the LSGD method with *dynamic node*, the comprehensive performance only attained medium levels among all other methods in most cases. This could be attributed to the fact that optimizing running time might also reduce the algorithm's performance in the precision-recall trade-off for specific experimental data. Therefore, implementation methods should be chosen based on the different focuses of algorithms.

V. CONCLUSIONS

In this paper, we present a novel appearance-based loop closure detection approach, SGIDN-LCD, that utilizes patch-level features extracted based-on Superior Grids and local region pixel intensities to represent images. We introduce the *dynamic node* framework to organize previously visited images and select candidate frames without the need to search through all images in the database. Qualitative and quantitative comparative experiments on different datasets demonstrate the superiority of our method over other state-of-the-art appearance-based LCD approaches in precision-recall evaluation. Experimental results show that introducing the *dynamic node* strategy and selecting appropriate parameters

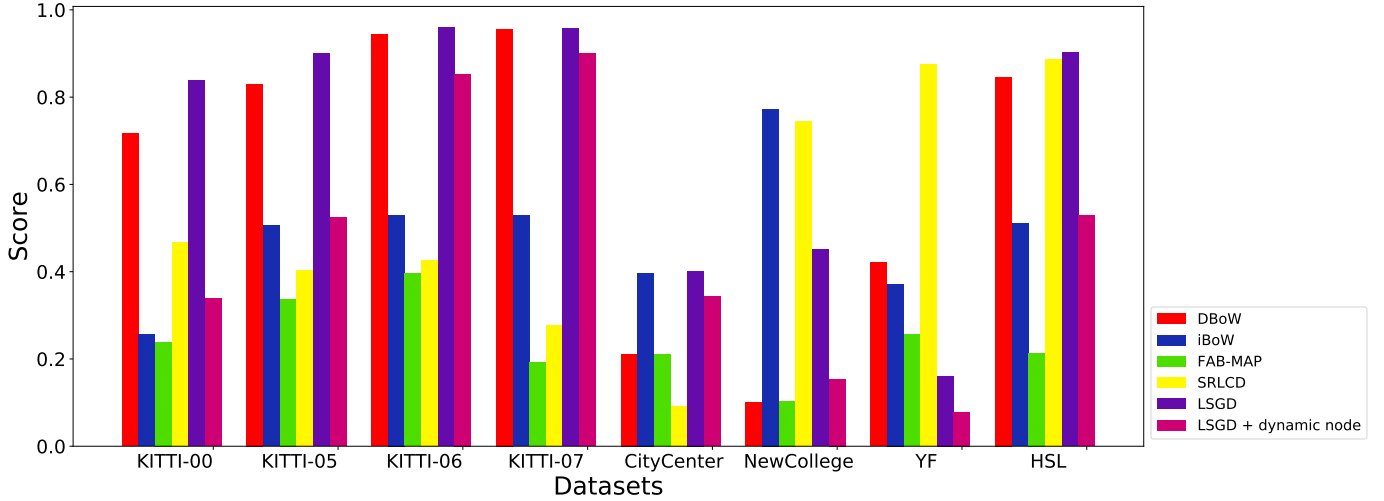


Fig. 6. The PRT evaluation for all LCD approaches on eight datasets. ($\omega = 10.0$)

can significantly reduce system processing time with only a minimal impact on precision and recall. In our future work, we plan to explore how to incorporate raw depth information from sensor inputs into our system to enhance the algorithm's understanding of the scene and improve the performance of loop-closure recognition.

REFERENCES

- [1] M. Calonder, V. Lepetit, C. Strecha, and P. Fua, "Brief: Binary robust independent elementary features," in *Computer Vision—ECCV 2010: 11th European Conference on Computer Vision, Heraklion, Crete, Greece, September 5–11, 2010, Proceedings, Part IV 11*, pp. 778–792, Springer, 2010.
- [2] E. Rublee, V. Rabaud, K. Konolige, and G. Bradski, "Orb: An efficient alternative to sift or surf," in *2011 International conference on computer vision*, pp. 2564–2571, Ieee, 2011.
- [3] X. Yang and K.-T. T. Cheng, "Local difference binary for ultrafast and distinctive feature description," *IEEE transactions on pattern analysis and machine intelligence*, vol. 36, no. 1, pp. 188–194, 2013.
- [4] P. F. Alcantarilla and T. Solutions, "Fast explicit diffusion for accelerated features in nonlinear scale spaces," *IEEE Trans. Patt. Anal. Mach. Intell*, vol. 34, no. 7, pp. 1281–1298, 2011.
- [5] H. Bay, T. Tuytelaars, and L. Van Gool, "Surf: Speeded up robust features," *Lecture notes in computer science*, vol. 3951, pp. 404–417, 2006.
- [6] D. G. Lowe, "Distinctive image features from scale-invariant keypoints," *International journal of computer vision*, vol. 60, pp. 91–110, 2004.
- [7] D. Nister and H. Stewenius, "Scalable recognition with a vocabulary tree," in *2006 IEEE Computer Society Conference on Computer Vision and Pattern Recognition (CVPR'06)*, vol. 2, pp. 2161–2168, Ieee, 2006.
- [8] E. Garcia-Fidalgo and A. Ortiz, "ibow-lcd: An appearance-based loop-closure detection approach using incremental bags of binary words," *IEEE Robotics and Automation Letters*, vol. 3, no. 4, pp. 3051–3057, 2018.
- [9] E. Garcia-Fidalgo and A. Ortiz, "On the use of binary feature descriptors for loop closure detection," in *Proceedings of the 2014 IEEE Emerging Technology and Factory Automation (ETFA)*, pp. 1–8, IEEE, 2014.
- [10] M. Cummins and P. Newman, "Fab-map: Probabilistic localization and mapping in the space of appearance," *The International Journal of Robotics Research*, vol. 27, no. 6, pp. 647–665, 2008.
- [11] P. F. Alcantarilla, A. Bartoli, and A. J. Davison, "Kaze features," in *Computer Vision—ECCV 2012: 12th European Conference on Computer Vision, Florence, Italy, October 7–13, 2012, Proceedings, Part VI 12*, pp. 214–227, Springer, 2012.
- [12] A. Angeli, D. Filliat, S. Doncieux, and J.-A. Meyer, "Fast and incremental method for loop-closure detection using bags of visual words," *IEEE transactions on robotics*, vol. 24, no. 5, pp. 1027–1037, 2008.
- [13] D. Gálvez-López and J. D. Tardos, "Bags of binary words for fast place recognition in image sequences," *IEEE Transactions on Robotics*, vol. 28, no. 5, pp. 1188–1197, 2012.
- [14] T. Nicosevici and R. Garcia, "Automatic visual bag-of-words for online robot navigation and mapping," *IEEE Transactions on Robotics*, vol. 28, no. 4, pp. 886–898, 2012.
- [15] S. Khan and D. Wollherr, "Ibuild: Incremental bag of binary words for appearance based loop closure detection," in *2015 IEEE International Conference on Robotics and Automation (ICRA)*, pp. 5441–5447, IEEE, 2015.
- [16] R. Arandjelovic, P. Gronat, A. Torii, T. Pajdla, and J. Sivic, "Netvlad: Cnn architecture for weakly supervised place recognition," in *Proceedings of the IEEE conference on computer vision and pattern recognition*, pp. 5297–5307, 2016.
- [17] A. Torii, R. Arandjelovic, J. Sivic, M. Okutomi, and T. Pajdla, "24/7 place recognition by view synthesis," in

- Proceedings of the IEEE conference on computer vision and pattern recognition*, pp. 1808–1817, 2015.
- [18] J. Sánchez, F. Perronnin, T. Mensink, and J. Verbeek, “Image classification with the fisher vector: Theory and practice,” *International journal of computer vision*, vol. 105, pp. 222–245, 2013.
 - [19] S. An, G. Che, F. Zhou, X. Liu, X. Ma, and Y. Chen, “Fast and incremental loop closure detection using proximity graphs,” in *2019 IEEE/RSJ International Conference on Intelligent Robots and Systems (IROS)*, pp. 378–385, IEEE, 2019.
 - [20] T. Naseer, L. Spinello, W. Burgard, and C. Stachniss, “Robust visual robot localization across seasons using network flows,” in *Proceedings of the AAAI conference on artificial intelligence*, vol. 28, 2014.
 - [21] M. Milford, E. Vig, W. Scheirer, and D. Cox, “Towards condition-invariant, top-down visual place recognition,” in *Australasian Conference on Robotics and Automation*, pp. 1–10, 2013.
 - [22] N. Sünderhauf, S. Shirazi, A. Jacobson, F. Dayoub, E. Pepperell, B. Upcroft, and M. Milford, “Place recognition with convnet landmarks: Viewpoint-robust, condition-robust, training-free,” *Robotics: Science and Systems XI*, pp. 1–10, 2015.
 - [23] P. Neubert and P. Protzel, “Local region detector+ cnn based landmarks for practical place recognition in changing environments,” in *2015 European Conference on Mobile Robots (ECMR)*, pp. 1–6, IEEE, 2015.
 - [24] C. L. Zitnick and P. Dollár, “Edge boxes: Locating object proposals from edges,” in *Computer Vision—ECCV 2014: 13th European Conference, Zurich, Switzerland, September 6–12, 2014, Proceedings, Part V 13*, pp. 391–405, Springer, 2014.
 - [25] B. Alexe, T. Deselaers, and V. Ferrari, “Measuring the objectness of image windows,” *IEEE transactions on pattern analysis and machine intelligence*, vol. 34, no. 11, pp. 2189–2202, 2012.
 - [26] S. Manen, M. Guillaumin, and L. Van Gool, “Prime object proposals with randomized prim’s algorithm,” in *Proceedings of the IEEE international conference on computer vision*, pp. 2536–2543, 2013.
 - [27] T. Malisiewicz and A. A. Efros, “Improving spatial support for objects via multiple segmentations,” in *Proceedings of the British Machine Vision Conference 2007, University of Warwick, UK, September 10–13, 2007*, 2007.
 - [28] R. Achanta, A. Shaji, K. Smith, A. Lucchi, P. Fua, and S. Süsstrunk, “Slic superpixels compared to state-of-the-art superpixel methods,” *IEEE transactions on pattern analysis and machine intelligence*, vol. 34, no. 11, pp. 2274–2282, 2012.
 - [29] A. Geiger, P. Lenz, and R. Urtasun, “Are we ready for autonomous driving? the kitti vision benchmark suite,” in *2012 IEEE conference on computer vision and pattern recognition*, pp. 3354–3361, IEEE, 2012.
 - [30] H. Wang, C. Wang, and L. Xie, “Online visual place recognition via saliency re-identification,” in *2020 IEEE/RSJ International Conference on Intelligent Robots and Systems (IROS)*, pp. 5030–5036, IEEE, 2020.